The Influence of Lightweight Concrete Ballast on Energy Conservation on Single-Ply Roof Systems

T.E. Phalen, Jr.

ABSTRACT

This research will develop surface temperatures on black roof surfaces during the warm cooling degree seasons in the New England area by means of actual field measurements. These measurements will be further compared to actual field temperatures on the top surface and underside of a 2-in-thick lightweight concrete ballast system. The field measurements will demonstrate black surface temperatures in the unprotected mode will reach values in excess of 190°F and will on the underside reach values equal to or in excess of ambient temperatures. The work will demonstrate that this developed temperature differential can reach values approaching 95°F.

This thermal approach, utilizing field temperature measurements, will be related to the dynamic response of the roof's insulating system to demonstrate substantial energy conservation utilizing field measurements. A simplified model will be developed that relates energy savings as a function of cumulative daily solar radiation, which demonstrates an energy consumption factor that is on the order of magnitude of 4500 Btu/ft^2/yr.

The work will further demonstrate that for refrigeration the energy savings now extend beyond the normal cooling degree day season with conservation features in the range of 1900 Btu/ft^2/yr when utilizing lightweight concrete ballast.

INTRODUCTION

The concepts relative to temperatures on surfaces that are exposed to the external environment (meaning the influence of the sun) are not new. Single-ply roof systems are a typical example of a relatively new type of construction that is exposed to the timeless external environment that includes the sun. These single-ply roof systems come in all types, from the ballasted variety (with all types of ballast stone and concrete pavers) to mechanically fastened and fully adhered systems. These single-ply systems utilize numerous types of membrane materials, such as EPDM, PVC, and Hypalon in a wide variety of colors (from stark white to black) that, with time, change in color. Each of these systems, however, is exposed to the same external factor—the sun—and, from a heat transfer consideration, each operates differently and produces substantially different influences on the heat transfer aspects of the design. These heat transfer aspects also influence the cost of energy associated with a given structure. This paper will develop basic data that will allow the designer to reasonably evaluate the cost of heating or cooling a structure with some of the single-ply roof systems.

In order to evaluate the performance of any single-ply roof system it is first necessary to obtain the surface temperature of the membrane. This, unfortunately, is not, on sunny and partly cloudy days, equal to the external ambient temperature. This external surface

Thomas E. Phalen, Jr. is Professor of Mechanical Engineering Technology, School of Engineering Technology, Northeastern University, Boston, MA 02115.

temperature is the equilibrium temperature of the roof's surface that is developed when the net rate of heat flow to and from the surface is equal to zero. Kreith (1965) was one of the first to demonstrate this basic criterion where the net heat flow to or from the body can be calculated by:

$$q_{net} = q_s + q_a + q_t + q_c + q_k - q_r \tag{1}$$

<u>where</u>

q_s = direct solar radiation absorbed

q_a = atmospheric radiation absorbed

q_t = terrestrial radiation absorbed

q_r = radiation emitted

q_k = net conduction to the body

q_c = net convection to the body

with all units being taken as Btu/h/ft^2, where q_t may be taken as zero since the surface does not see any part of the earth and, further, q_k=0. Also, on a sunny day (according to Kreith), q_a may be taken as $q_a \approx 0.1\ (q_s)$:

$$q_s + q_a \approx 1.1\ q_s \tag{2}$$

Then, from Equation 1

$$1.1\ q_s + q_c + q_k - q_r = 0 \tag{3}$$

where q_r may be approximated, according to Kreith, by

$$q_r = 1.71 \times 10^{-9}\ \varepsilon\ T_s^4 \tag{4}$$

and q_c is given by

$$q_c = h_c(T_s - T_a) \tag{5}$$

where temperatures are in absolute units as shown hereinafter.

Using the Kreith (1965) approach for q_s for low-slope roofs (<1/4 in/ft) it can be shown that

$$q_s = 309\ \alpha_s \cos Z \tag{6}$$

where z is the angle that the sun's rays make with the vertical and α_s is the absorptivity of the surface from solar radiation. For the maximum surface temperature under solar conditions, z may be approximated as 90°. Then the approximate maximum equilibrium temperature similar to the Kreith approach may be written as

$$309\ \alpha_s = 1.71 \times 10^{-9}\ \varepsilon\ (460+T_s)^4 + h_c(T_s - T_a) \tag{7}$$

For stagnant conditions on a clear day h_c for air will vary over a small range; however, for the temperature range involved, the value of h_c may be taken as about 0.62. Thus, the maximum equilibrium temperature, T_s, becomes solely a function of α_s, ε, and the ambient temperature (T_a). Thus, Equation 7 demonstrates from very fundamental classic theory and concepts that the equilibrium temperature of any material that is exposed to natural sun is a function solely of certain fixed constants, namely the absorbtive and emitive characteristics of the surface of the material exposed to the sun. <u>These basic concepts are often minimized and neglected in the single-ply roof industry</u>.

It is interesting to note that Equation 7, as developed from Kreith's original work in the 1950s, is identified in form as the fundamental equation utilized by Wilkes (1988) in establishing a computerized model for the analysis of the impact of naturally induced high temperatures on roofs.

One of the first studies relating to the concept outlined in Equation 7 was presented by Dunkle and Gier (1957). This work, related to equilibrium surface temperatures for many different surfaces as a function of time and external temperature, is shown in Figure 1.

This work clearly demonstrates that on a day when exterior temperatures ranged from 61° to 70°F flat black surfaces reached a temperature of 115°F in comparison to a white surface, whose maximum temperature was about 69°F, while other "gray" surfaces were higher than the white surface, but substantially less than the black surface.

By identifying the absorptivity and emissivity factors related to the radiant heat transfer mechanism this early work also enabled investigators to identify factors that influenced emissivity. Two key factors other than color indicate a major influence on emissivity. These factors are surface roughness (polished or rough) and the air content of the surface material. Roughness and air content of the surface material, as in lightweight concrete, have yet to be clarified as to combined overall influence.

Since the mid-1950s, the influence of "white" surfaces has been nicely summed up by Kreith (1965). "This property can be used to advantage on roofs in a sunny climate, where it is desirable to keep the roof temperatures as low as possible for the comfort of the occupants." For whatever reason, the recent advent of single-ply roofs of all sorts, particularly the exposed membrane types, appears to have basically discarded the well-known energy-related factors noted before. Recently, numerous fully adhered and mechanically fastened roof systems have been installed with little or no thought relative to the heat transfer characteristics of these "black" single-ply roof systems. Thus, the work in this paper will be guided toward identifying some key parameters relative to the impact of black single-ply exposed roof membranes to heat transfer and energy-related matters.

TYPICAL SINGLE-PLY ROOF SYSTEMS AND EXTERNAL SURFACE TEMPERATURES

A typical single-ply roof system that is either mechanically fastened or fully adhered will be placed in the configuration shown in Figure 2.

In many cases the membrane installed is a black EPDM membrane ranging in thickness from 45 to 60 mil (1 mil=0.001 in). Thus, the external ambient temperature for design purposes is taken to be between 95° and 100°F (in summer months) and -10° to 10°F in winter months in general for the United States, with an internal nominal temperature for human habitation around 70°F. Further, the heat transfer condition for normal design is commonly taken in the roofing industry to be the steady one-dimensional heat flow for a plane surface or

$$q = \frac{kA(T_A - T_i)}{L} = \frac{A(T_A - T_i)}{L/k} = \frac{A(T_A - T_i)}{R} \tag{8}$$

When utilizing a black EPDM membrane, Equation 7 suggests that on sunny or even on partially sunny days the surface temperature (T_s) will be substantially higher than external temperature T_A in Equation 8. Further, this increase in T_A to T_s suggests a major increase in heat gains while at the same time the heat transfer becomes a dynamic situation rather than the steady-state condition of Equation 8.

Whether the heat transfer aspect of the system is the steady or transient state, the first segment of the problem is defined by the magnitude of the outside surface temperature and the length or period of time that the temperature exists. High temperature over a short period of time in itself is not detrimental; however, high temperatures over the period of daylight hours have been demonstrated by Wilkes (1988) and Griggs (1988) to substantially influence cooling loads. Thus, in order to examine this aspect, a series of simple temperature vs. time measurements were conducted to verify surface temperatures vs. time factors.

Recognizing that the single-ply industry does utilize exposed black EPDM membranes as large segments of single-ply roofs currently being installed as mechanically fastened systems and single-ply EPDM membranes ballasted with heavyweight and lightweight ballast units as well as stone ballast, a series of surface temperature measurements were made so that direct comparisons of various surfaces could be made. The initial measurements were made on plain exposed EPDM membranes and EPDM membranes ballasted with heavyweight (26 psf)(t=2 in) and lightweight concrete ballast units (12 psf)(t=2 in), installed on extruded polystyrene insulation on a concrete deck with a controlled internal temperature with measurements being made by a series of thermocouples recording simultaneous surface membrane temperatures and ballast surface temperatures. Figure 3 represents a typical series of surface temperatures along with ambient temperatures. The results of Figure 3 clearly demonstrate that fully exposed black EPDM does absorb energy in a fashion predictable by Equation 7 and that this surface temperature approaches 190°F during summer months in northern latitudes (i.e., Boston, MA). The results further indicate that conventional heavyweight ballast units have temperatures that are about 150°F and tapered lightweight interlocking concrete ballast units (LWICB) have surface temperatures approaching 130°F when the ambient temperature is about 95°F. Again, these latter units also follow "gray body" concepts of Equation 7. Further, the results indicate that the surface temperatures exceed a 95° exterior design temperature for a period of about eight to nine hours for the black EPDM. The use of ballast units clearly reduces the surface temperature influence substantially. Also, the elevated temperature of exposed black EPDM is high and occurs for a long period of time.

Figure 4 compares the top and bottom temperatures of two ballast systems to the black EPDM surface temperatures. These results clearly indicate that the ballast units provide a protective element for the roof's surface from high temperatures. The LWIC system changes the surface temperature of the membrane by 73°F and the heavyweight unit by 62°F. These numbers by themselves must be considered significant from a thermal design viewpoint.

Figure 5 represents a typical surface temperature vs. time condition for an LWIC unit in the winter months. This demonstrates that the surface influence during winter months follows the same pattern as the summer but to a lesser degree.

Further, Figures 3, 4, and 5 demonstrate that a substantial influence on the heat flow characteristics must occur during the summer months when the external temperatures that are influencing the surface temperature of the insulation are maximized (i.e., 140°F to 190°F). This indicates that the high surface temperature conditions applied during an 8- to 12-hour period must transmit, in a transient or dynamic condition, sufficient heat to materially influence energy consumption. If the energy consumption turns out to be relatively small, then the influence of high surface temperatures becomes academic and not of practical concern. This aspect of the problem can be viewed theoretically by considering the insulation to be an infinite flat plate being subjected to a variable surface temperature induced by solar heat. Within the roofing industry there exists a large segment of professionals that view model calculations with skepticism. For this reason, and for the reason that the mathematical approach to the solution is intricate, the solution to this aspect of the problem will originate with field measurements that will be tied to well-known simple basic concepts and developed hereinafter.

INSULATION ASPECT

Clearly the previous discussion and experimentation has demonstrated that the surface temperature of the roof insulation is a function of the materials above the membrane. This discussion also clearly demonstrated that the insertion of a ballast layer substantially reduces the surface temperature of the insulation and that the LWIC ballast produced the lowest results. The answer to how much heat is gained in the summer months now becomes a function of the dynamic heat transfer aspects of the insulation. Unfortunately the number and types of insulation utilized in the roofing industry is large and no one single insulation has penetrated the market to gain the lion's share. This makes the selection of insulation for testing purposes difficult. Since polystyrene insulations are popular, occupy a fair percentage of the market, and have thermal properties that represent the lower value of insulations reasonably well, extruded polystyrene was selected as the prototype insulation for the tests within this report. Two and four inches of extruded polystyrene were established with thermocouples measuring temperatures on the top, midplane, and bottom of the insulation. The surface temperature was then monitored for various external conditions with corresponding midplane and bottom temperatures. Figure 6 is a typical result of this temperature monitoring. These data clearly indicate that the insulation does absorb heat. Further, the temperature of the bottom surface does rise substantially above the ambient internal temperature. This factor clearly identifies the simple fact that the insulation does absorb radiant energy and that this radiant energy in part passes through the insulation and is transmitted to the interior environment and thus could have the potential to influence the conditioning of the internal environment.

Further measurements of the surface temperature over ranges from about 100°F to 190°F and the bottom interior temperature were conducted. These results are shown in Figure 7.

Analysis of the data in Figure 7 indicates that the differential temperature between the top (T_{o_s}) and bottom (T_{i_4}) surface for the 4 in of extruded polystyrene insulation takes the following form

$$T_{i_4} = T_{o_s} - 0.1378T_{o_s}^{1.218} \approx 1.213T_{o_s}^{0.855} \tag{9}$$

The data for Equation 9 are based upon a thickness of 4 in of insulation. Unfortunately, commercial and industrial structures generally utilize only 2 in of insulation. Figure 8 represents this condition. The data relative to surface temperature and bottom temperature are also included in Figure 7. The relationship of top (T_{o_s}) and bottom (T_{i_2}) temperatures for the data shown in Figure 7 for 2 in of extruded polystyrene may be written as

$$T_{i_2} = T_{o_s} - 0.0497T_{o_s}^{1.35} \approx 1.382T_{o_s}^{0.867} \tag{10}$$

The data for surface temperatures of black EPDM with a plain surface, surface temperature with normal heavyweight ballast units (HWC), and lightweight interlocking concrete pavers, as previously shown in Figures 3, 4, and 5, can be represented as a function of the ambient temperature for a cloudless day, as shown in Figure 9.

The results in Figure 9 take the form of

$$T_s = AT_A^B \tag{11}$$

where the values of A and B are shown in Table 1.

When the results of Equations 9 and 10 are combined with Equation 11, the temperature of the bottom of the insulation can now be written in the form of

$$T_i = T_s - CT_s^D \tag{12}$$

Inserting Equation 11 yields an equation for the bottom temperature of the insulation that takes the general form of

$$T_i = A_1T_A^{B_1}(1-C_1T_A^{D_1}) \tag{13}$$

where the values for A_1, B_1, C_1, and D_1 for various conditions are given in Table 2.

Also shown in Table 2 is the computed temperature (T_i) of the inside or bottom surface of the insulation based upon field measurements for a clear day when the ambient temperatures are 100°F and 85°F, respectively. These results indicate that the temperature on the bottom side of the insulation is comparatively high, clearly indicating that solar energy is substantially contributing to the cooling load for both insulation thicknesses (2 and 4 in). Further, the ballast units are substantially reducing the influence of solar energy and the LWIC ballast unit clearly exhibits a substantial impact on conservation of energy related to solar energy.

ENERGY CONSIDERATIONS

The previous results were simply related to establishing the temperatures induced at various key locations in the roof system when exposed to solar radiation. These results clearly indicate that solar energy is influencing the heat transfer aspects of the roof system during the warmer summer months. This section of this research will establish criteria for the evaluation of the heat gain from solar energy.

The beginning of evaluating these heat gains is related to the thermal conductivity and thickness of the insulation within the roof system. Unfortunately, roof insulation covers a very broad spectrum of materials. The types of insulation that have the lowest coefficients of thermal conductivity, as noted by Dechow and Epstein (1977), are fiberglass, polystyrene, and urethane-type insulations. This early work and work of other later investigators has clearly demonstrated that foam-type insulations do lose insulating values as a function of time--all of which is not accountable from increase in moisture. This work indicated that these insulations commence with coefficients of thermal conductivity ranging from 0.016 to 0.04 W/m·K and, after 8 to 10 years of service, increase to 0.03 to 0.06 W/m·K. Further, these roof insulations are substantially influenced by moisture, further increasing the coefficient of thermal conductivity. The conversion factor to convert W/m·K to Btu/h/ft^2/°F is 0.578. Applying the conversion factor indicates that the lowest coefficient of thermal conductivities in service would be on the order of magnitude of 0.2 to 0.3 Btu/in/h/ft^2/°F. These factors indicate that "real world" heat gains will vary over a wide range and that a test insulation that has a thermal conductivity of 0.2 to 0.3 Btu/in/h/ft^2/°F will establish a reasonable low data base for the influence of solar energy on roof systems.

In their study, Dechow and Epstein (1977) evaluate insulations on a semi-international basis from North America to Europe. This evaluation included 43 case studies. The median insulation thickness for the 46 cases evaluated was 1.6 in with a standard deviation of 0.52. This indicates and concurs with the writer's observations that the average thickness of insulation being utilized in ordinary structures lies between 1 1/2 to 2 in. For this reason and the other facts noted at the beginning of this section, the insulation thicknesses utilized for study purposes were 2 and 4 in with a k-value of about 0.25 Btu/in/h/ft^2/°F (as indicated by Dechow and Epstein (1977)) and recognizing that "real world" data would probably be related to thicknesses of 2 in of insulation.

The previous factors indicate that the heat gain must become a function of insulation thickness and solar energy absorbed by the surface. This concept has been recognized by the engineering profession for many years. Strock and Koral (1959) published time-tested material relative to heat gains from solar energy. These data took the form of

$$H = AIbg \tag{14}$$

Utilizing the empirical data presented from solar maps by Strock and Koral, Equation 14 may be rewritten as a function of R and T_A for H in Btu/ft^2/h or

$$H = 15.02(b)\,\frac{1}{R}^{1.0355}\,(T_A)^{0.313} \tag{15}$$

Within the roofing industry 2 and 4 in of foam-type insulation is generally accepted as being equivalent to R values of 10 and 15, respectively. Utilizing R-values of 10 and 15, combined with an ambient temperature of 98°F for a black EPDM membrane, yields H-values of 5.5 and 3.6 Btu/ft^2/h. These values yield an approximate preliminary value for H.

Numerous experimental procedures have been conducted at a national laboratory to develop in situ heat fluxes for various types of roof systems utilizing calibrated heat transducers. Heat flux results have been reported by Wilkes (1988), Griggs (1988), and Courville and Beck (1988). These results are compatible with results from the empirical approach of Equation 15. Figure 10 represents a typical result from the national laboratory test procedure developed by Courville (1989) for midplane heat flow for the LWIC system utilizing 12 psf lightweight units identical to those utilized in this report with 4 in of expanded polystyrene insulation when the temperature reached 95°F. These data, developed utilizing extremely sophisticated instrumentation in 1987, are yielding data that are totally compatible with initial concepts developed in the early 1950s. These data have simply reinforced original concepts. These data confirm the fact that a heat gain during the summer months is taking place for about a 12-hour period and that the area under the heat flow curve (approximately a simple triangle) allows for the computation of the daily heat gain. For the case shown in Figure 6, the total heat gain on a 95°F clear day is about 20 to 32 Btu/ft^2/day.

Utilizing simple calorimeter techniques with distilled water in the calorimeter, the writer also conducted a series of heat flow experimental procedures. The approach yielded good results for the period when the temperature was rising to the maximum values. These results were then related to the bottom surface temperature of the insulation. The results of this work are shown in Figure 11, where the bottom-side temperature was related to the heat flux.

The results depicted in Figure 11 yield the following relationship:

$$H = 0.0408T_i^{0.9685} \tag{16}$$

Equation 13 may now be substituted into Equation 16, yielding

$$H = 0.0408\, A_1 T_A^{B_1} (1-C_1 T_A^{D_1})^{0.9685} \tag{17}$$

Equation 17, utilizing the constants developed in Table 2, may be utilized to evaluate the maximum heat flow (i.e., heat gain) for various exterior conditions on a clear day. These results are shown in Table 3.

The results of Table 3 are consistent with results obtained by the empirical approach of Equations 14 and 15. Griggs (1988) presents data on the cumulative heat flux for black and white surfaces with 4 in of polystyrene insulation. Griggs' results for the maximum and daily heat flux can be expressed for the white and black surfaces as

$$\Sigma Q_W = 1.161(t_2-t_1) \tag{18a}$$

and

$$\Sigma Q_B = 3.244(t_2-t_1) \tag{18b}$$

where (t_2-t_1) represent either 1 hour or a 12-hour time interval. Equations 18a and 18b yield heat fluxes for a 1-hour period ranging from 1.2 to 3.2 Btu/ft^2, which is compatible with the data in Table 3 and for a 12-hour period (1 day) ranging from 14 to 39 Btu/ft^2/day. This is compatible with the results noted previously for Figure 6. This indicates that the results of this work and work by others are basically yielding similar results.

APPLICABLE SOLAR TIME AND TOTAL SOLAR GAIN

Previous work has demonstrated that the heat gain from solar energy is a complex problem. The work has further demonstrated that solar energy gains for each roof system are a function of the type of insulation and its thickness. The work has also demonstrated that the magnitude of the heat gain on a given day is measurable by empirical techniques developed by Strock and Koral (1959) and has been verified experimentally by work at a national laboratory and by the work developed in this paper. Unfortunately, the evaluation of the total annual heat gain also is not a straightforward calculation for the simple reason that "mother nature" does not supply a constant amount of solar energy daily. The variation in solar energy for sunny days, however, has been evaluated by the U.S. Weather Bureau (Fritz et al., n.d.) and is presented in Strock and Koral (1959). The cumulative variation of solar energy for any geographic location in the United States as a function of time takes the form shown in Figure 12. Figure 12 depicts the cumulative solar radiation as a function of time for Boston, MA, and Miami, FL, with zero time designated as January 1 of a given year. Solar energy begins to influence the internal temperature when the cumulative solar energy is about 900 and 1300 Langleys in Florida and New England, respectively. These values were obtained from comparisons of weather data in Strock and Koral (1959) and Fritz et al. (n.d.). The time in days when the solar gains in Boston and Miami can be estimated by Equations 18a and 18b, respectively, or

$$n_M = 365-2(0.304)H_1^{0.784} \qquad \text{(239 days Miami)} \tag{19a}$$

$$n_B = 365-2(0.669)H_1^{0.699} \qquad \text{(164 days Boston)} \tag{19b}$$

The total heat flow from solar radiation, ΣQ, developed is given by

$$\Sigma Q = nQ_m \tag{20}$$

where Q_m is the maximum solar heat flow for a day, and n is the number of days in which this flow takes place. The experimental work done in this research indicated that for a given day, the solar heat flux took the form shown in Figure 13c. Further, the maximum daily solar heat flux, Q_m, influenced the heat gain for a daily period of time (t') and for the configurations tested, the relationship between influence time t' and the solar heat flux could be written as (and is shown in Figures 13a and 13b)

$$t' = 5.4Q_m^{0.7523} \tag{21}$$

Recognizing the shape of the heat flux for a given day, Equations 20 and 21 may be utilized to develop a conservative evaluation of the total yearly solar influence or

$$\Sigma Q = nQ_m = \frac{n}{2}\frac{t'Q_m}{2} = 1.35nQ_m^{1.752} \tag{22}$$

Utilizing Equation 22 with the measured results in Table 3 leads to the annual heat gains (i.e., increase in air-conditioning load) that can be attributed for a system in Miami, FL. These results are noted in Table 4.

The results shown in Table 4 clearly demonstrate that the heat gain from an exposed EPDM roof is substantial in magnitude and that the influence of solar heat gain is substantially reduced by the ballast system.

It should be recognized that Table 4 is based upon Equation 22 and is a methodology for estimating the influence of solar energy on various types of single-ply roof systems. Since the initial draft of this work, the writer reviewed a document being developed for estimating the influence of solar reflectance on low sloped roofs. Computations utilizing the Griggs et al. (1989) approach and comparing these values to Table 4 yield very compatible values. This comparison clearly demonstrates that Equation 22 yields reasonable values for solar gains but, more important, demonstrates that heat gains from solar reflectance on single-ply roof systems is a major thermal design consideration.

CONCLUSIONS

The results developed in this paper indicate that the actual heat gain from solar radiation is a complex function of many variables and can be expressed as

$$q = f(\alpha_s, t, T_A, k, h_c, I, Z) \tag{23}$$

The work further demonstrates that relatively simple field measurements can be utilized to investigate the impact of the numerous variables on the heat transfer aspects in single-ply roof systems.

The research further confirms that surfaces of roofing systems such as exposed black EPDM exceed a temperature of 190°F on clear sunny days and that this substantial rise in surface temperature, as predicated by early theory relative to radiation, has been verified by simple field measurements. The work further demonstrates that for a given insulation system, the heat flux through the system can be described as a function of the inside surface temperature of the insulation and can be related to the exterior ambient temperature. The work demonstrates that plain exposed black EPDM roof systems develop substantial heat gains during summer months as a result of solar energy and this energy gain is significant. Further, the work also indicates that the use of a lightweight concrete ballast system does substantially reduce membrane temperatures, insulation temperatures, and heat flux. Of greater importance, the work demonstrates that black single-ply surface temperatures reach very high temperatures during large portions of the year.

SYMBOLS

A = Area (ft^2)

A, B, C, D = empirical constants (subscripts A_1, etc. designate a different empirically developed constant)

b = decimal part of solar radiation absorbed by surface

g = decimal part of b transmitted to inside

H_i = cumulative solar radiation (langley's)

H = sun heat reaching the room (Btu/h/ft^2)

h_c = conductance (Btu/h/ft^2/°F)

I = intensity of solar radiation (Btu/h/ft^2)

k = coefficient of thermal conductivity (Btu-m/ft^2-h-°F)(W/m/°K)

L = thickness (ft or in)

n = number of days

Q_m = measured maximum solar heat flux (Btu/ft^2)

ΣQ = yearly heat gain (Btu/ft^2/yr)

q = heat flow to or from a body (Btu/h/ft^2)

q_a = atmospheric radiation absorbed (Btu/h/ft^2)

q_c = net convection to the body or surface (Btu/h/ft^2)

q_k = net conduction to the body (Btu/h/ft^2)

q_r = radiation emitted (Btu/h/ft^2)

q_s = direct solar radiation absorbed (Btu/h/ft^2)

q_t = terrestrial radiation absorbed (Btu/h/ft^2)

R = thermal resistance (h/ft^2/°F/Btu)

T_A or T_a = ambient temperature (°F)

T_{os} = surface temperature of insulation (°F)

T_o = outside temperature (°F)

T_i = bottom surface temperature of insulation (°F) (also inside temperature)

t = time (h)

t' = solar base time (h)

Z = angle sun's rays make with the vertical

ε = emissivity for radiation

α_s = absorptivity for Radiation

Conversion Factors = Btu/in/ft^2/h = 0.1442 W/mK

Btu/ft^2 = 1.136 W/m^3

Btu/h = 0.293 W

REFERENCES

1. Courville, G.E. 1989. "Data reduction from Oak Ridge National Laboratory." Private correspondence, Oak Ridge, TN, January 26.

2. Courville, G.E., and Beck, J.Y. 1988. "Measurement of field thermal performance of building envelope components." Oak Ridge National Laboratory, Oak Ridge, TN.

3. Dechow, F.J., and Epstein, K.A. 1977. "Laboratory and field investigations of moisture absorption and its effect on thermal performance of various insulations." Thermal Transmission Measurements of Insulation, ASTM STP660, Philadelphia, PA, September.

4. Dunkle, R.V., and Gier, J.T. 1957. "Selective spectral characteristics of solar collectors." Trans. Tuscon Conference on Applied Solar Energy, Vol. 2.

5. Fritz, S.; MacDonald, T.H.; and Hand, I.F. "Daily total solar energy," and "Solar energy received on horizontal surfaces." U.S. Weather Bureau, various years.

6. Griggs, E.I. 1988. "Modeling how a roof's reflectance affects thermal performance." Mathematical Modeling of Roof Systems Symposium, Roof Research Center, Oak Ridge National Laboratory, Oak Ridge, TN, September.

7. Griggs, E.I.; Sharp, T.R.; and MacDonald, J.M. 1989. "Guide for estimating differences in building heating and cooling energy due to changes in solar reflectance of a low-sloped roof." Final Draft, Office of Buildings and Community Systems, Oak Ridge National Laboratory, Oak Ridge, TN, ORNL/CON-Draft-04/89.

8. Kreith, F. 1965. Principles of Heat Transfer. Scranton, PA: International Textbook Co.

9. Strock, C., and Koral, R.L. 1959. Handbook of Air Conditioning Heating and Ventilating. New York: The Industrial Press.

10. Wilkes, K.E. 1988. "A model to predict heat flows and temperatures in roofs." Mathematical Modeling of Roof Systems Symposium, Roof Research Center, Oak Ridge National Laboratory, Oak Ridge, TN, September.

TABLE 1

Constants A and B for Equation 11

Condition	A	B
Plain Exposed EPDM	7.218	0.712
HWC	2.93	0.8312
LWIC	0.940	1.072

TABLE 2

Values for A1, B1, C1, and D1 in Equation 13 for Various System Conditions
(T_i = Bottom of Insulation With Deck)

Condition	Insulation Thickness	A_1	B_1	C_1	D_1	Ti When (T_A=100°F)	Ti When (T_A=85°F)
1-Plain EPDM	4	7.22	0.712	0.212	0.155	108.7	98.7
2-HWC	4	2.93	0.831	0.174	0.181	80.7	71.8
3-LWIC	4	0.94	1.072	0.136	0.233	78.8	67.9
4-Plain EPD	2	7.22	0.712	0.0993	0.249	131.8	119.5
5-HWC	2	2.93	0.831	0.0724	0.291	97.3	86.5
6-LWIC	2	0.940	1.072	0.0486	0.375	95.2	81.7

TABLE 3

Heat Gain for Various Conditions (Equation 17)

Condition	Insulation Thickness (in) (T_A=95°F)	H(Btu/ft^2/h) (Maximum)
Plain EPDM	2	4.5
HWC	2	3.3
LWIC	2	3.2
Plain EPDM	4	3.7
HWC	4	2.8
LWIC	4	2.7

TABLE 4

Annual Solar Heat Gain Miami, Florida (Developed from Equation 22)

Condition	Insulation Thickness (in)	Q(Btu/ft^2/yr)
Plain EPDM	4	3200
HWC	4	1950
LWIC	4	1840
Plain EPDM	2	4500
HWC	2	2610
LWIC	2	2480

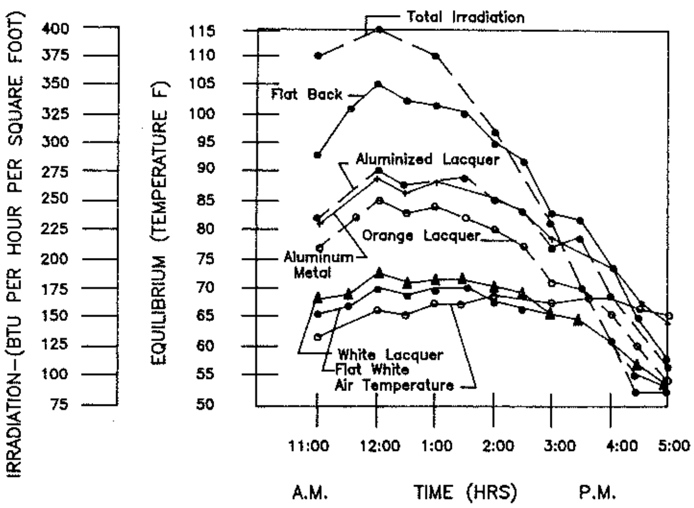

Figure 1. *Irradiation and equilibrium temperature versus time*

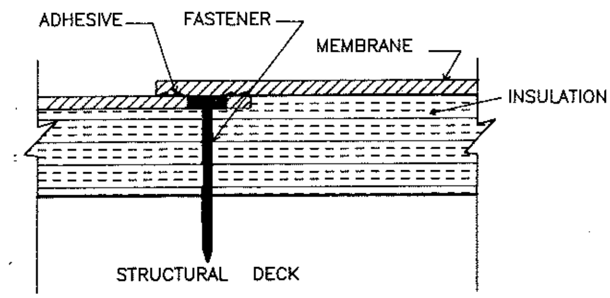

Figure 2. *Roof cross-section*

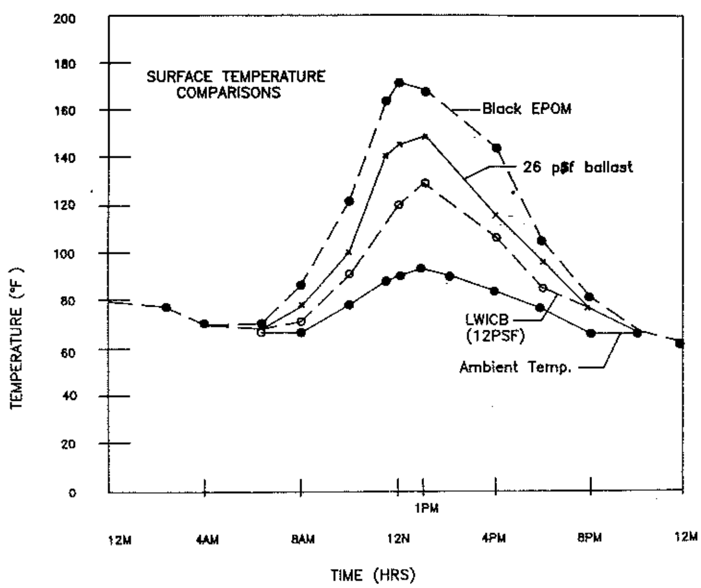

Figure 3. *Surface temperature comparison*

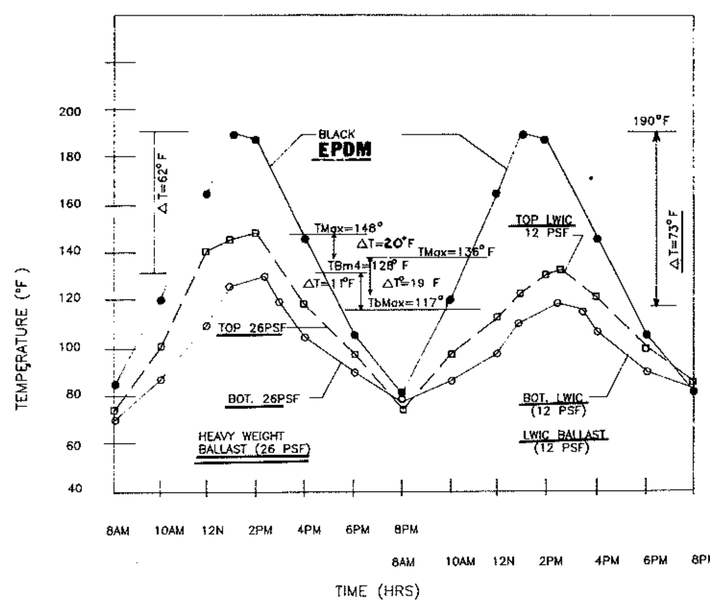

Figure 4. *Temperature versus time for EPDM and concrete ballast units*

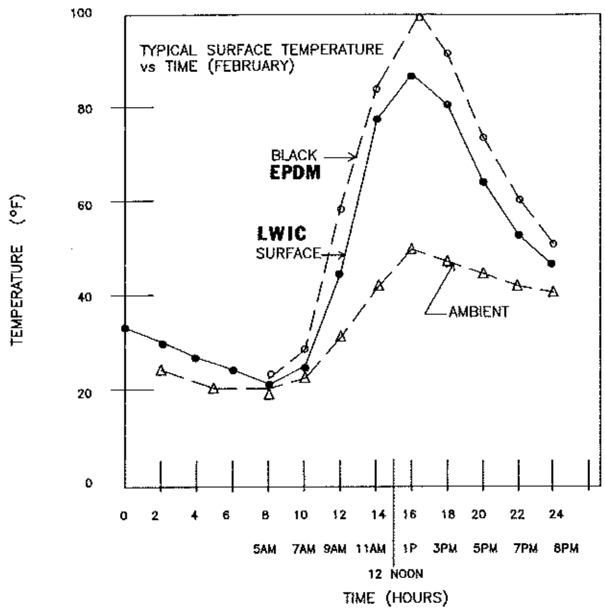

Figure 5. Typical surface temperatures versus time (February)

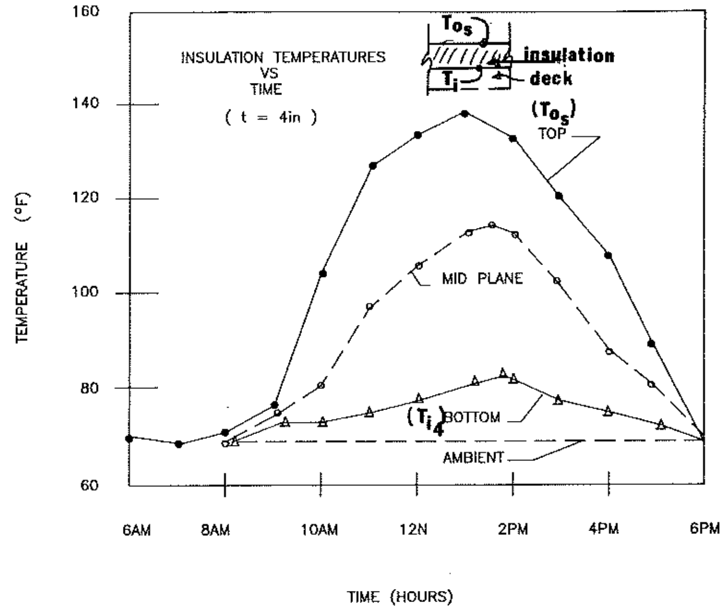

Figure 6. Insulation temperatures versus time

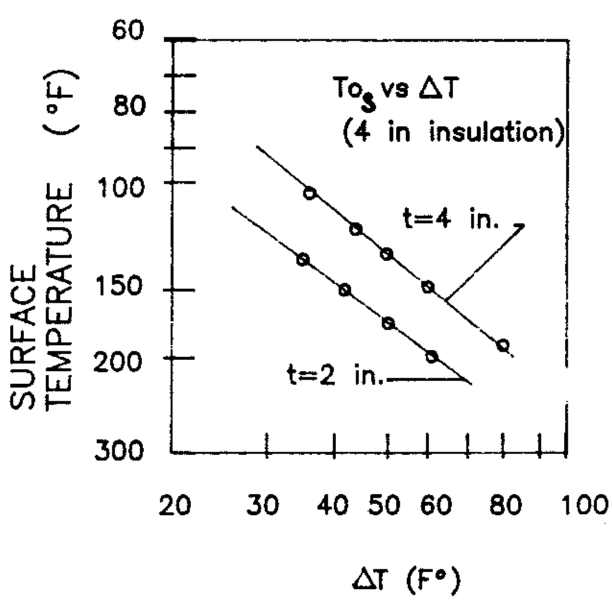

Figure 7. Surface temperature versus differential temperature for 2-inch and 4-inch insulation

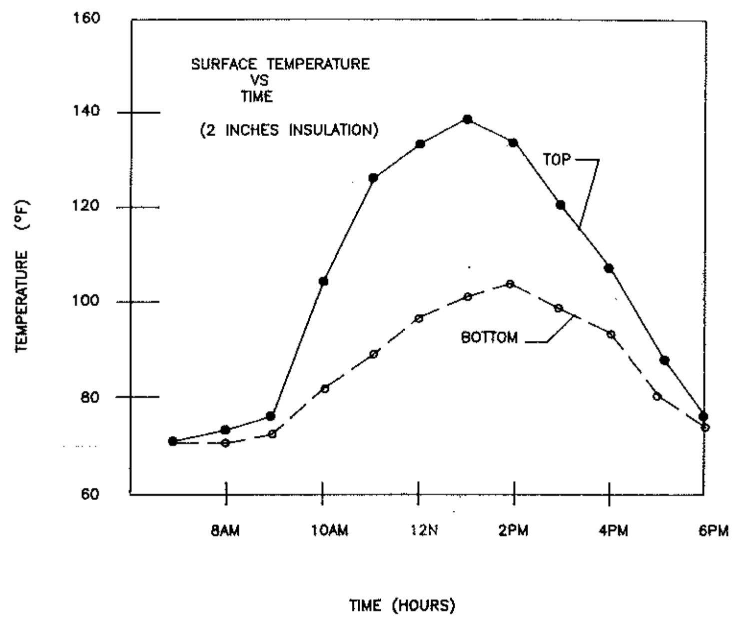

Figure 8. Surface temperature versus time for 2-inch insulation

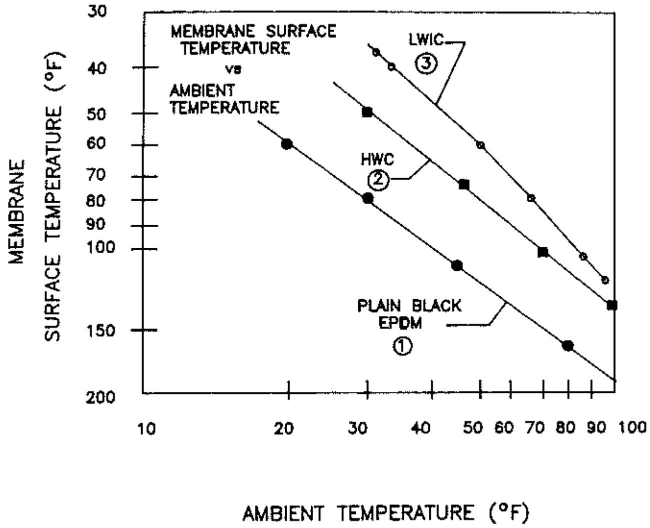

Figure 9. Membrane surface temperature versus ambient temperature

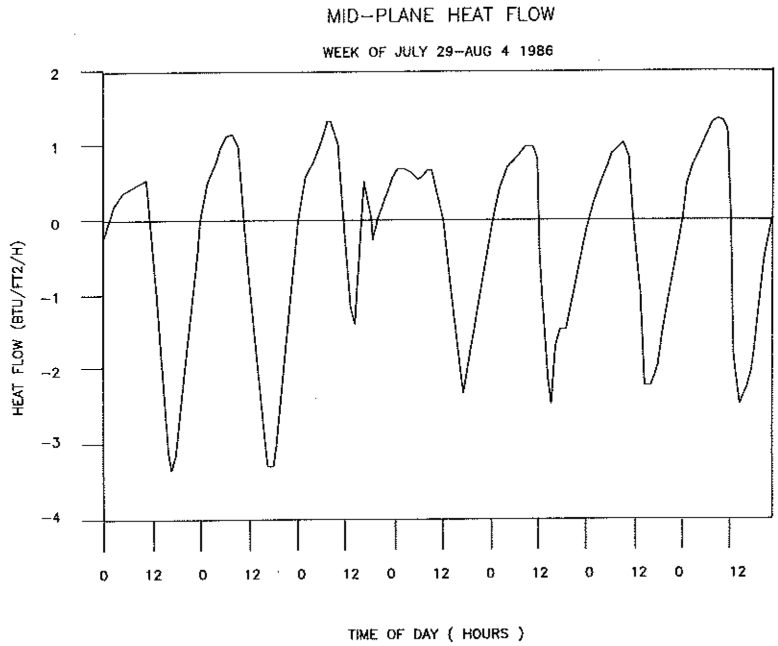

Figure 10. Mid-plane heat flow

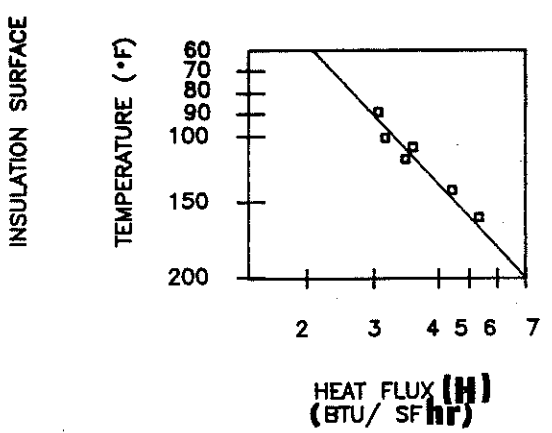

Figure 11. Insulation surface temperature versus heat flux

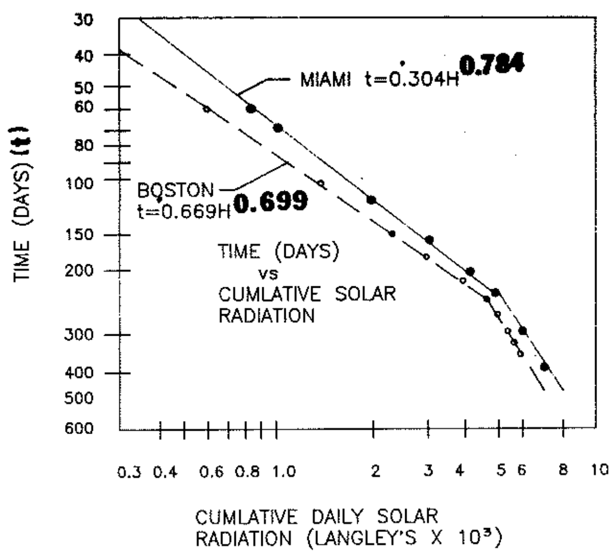

Figure 12. Time versus cumulative daily solar radiation (Miami and Boston)

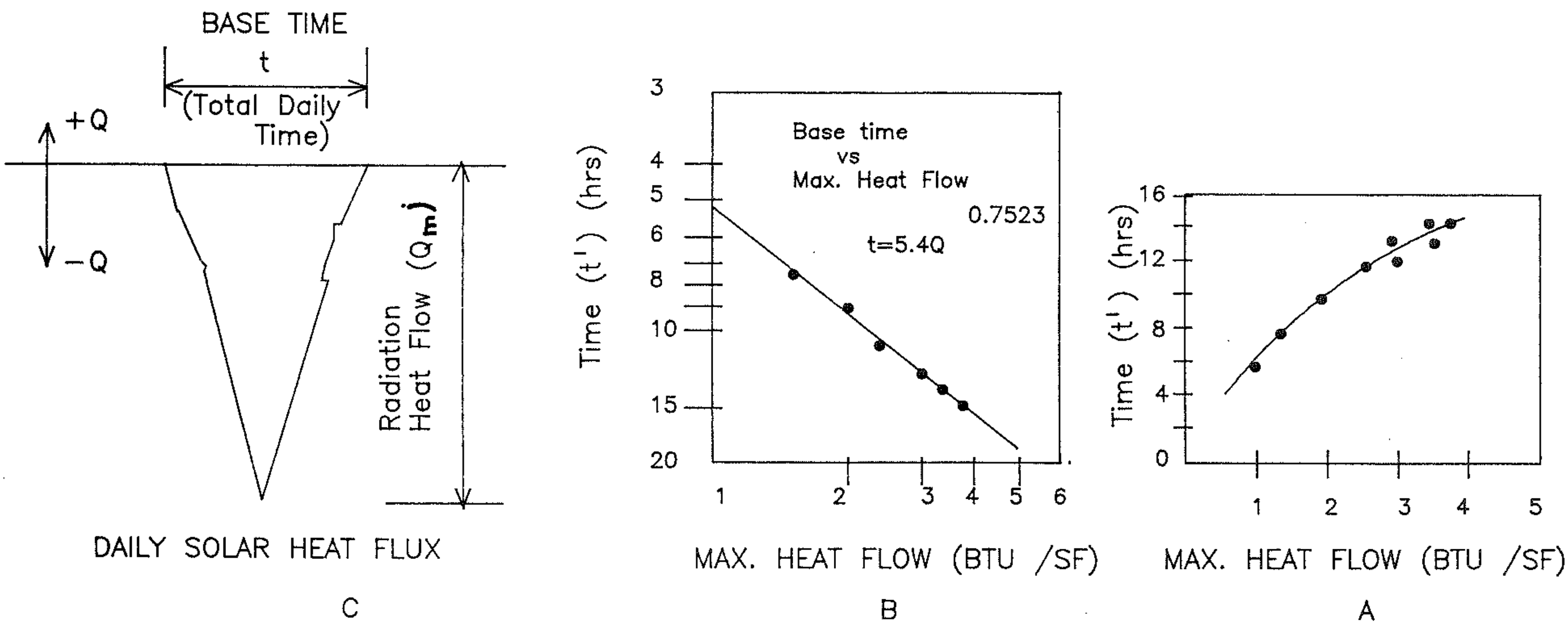

Figure 13. Solar heat flux versus time